SIAM J. APPL. MATH.
Vol. 61, No. 1, pp. 22–42

MODELING INJECTION MOLDING PROCESSES WITH DEFORMABLE POROUS PREFORMS*

D. AMBROSI† AND L. PREZIOSI†

Abstract. This paper deduces a new model aimed at simulating injection molding processes under isothermal conditions. These processes can be generally stated as infiltration problems in initially dry porous materials. The spatial domain is then divided by the infiltration front into two time-dependent subdomains, the dry and the wet porous preforms, both being allowed to deform under the action of the liquid pressure. It is shown that the model calls for the definition of the stress-deformation relationship of both the dry and the wet preforms, which are assumed to behave elastically and inelastically, respectively. The coupled flow/deformation problem in the two regions (separated by an interface) is formulated with the corresponding boundary conditions and with the proper evolution equations determining the motion of the boundaries.

The mathematical problem is solved numerically, highlighting the importance of inertial terms in the early stage of the infiltration and focusing on the influence of the mechanical properties of the material and on the deformation of the preform during the infiltration process.

Key words. analytical modeling, injection molding, resin transfer molding (RTM), deformable porous media

AMS subject classifications. 33H40, 35C01

PII. S0036139998333671

1. Introduction.

The possibility of using composite materials in more and more technological applications is generating an ever growing interest in improving manufacturing processes by the development of suitable mathematical models. In particular, increasing attention is being paid to those processes which can be classified as injection molding methods. This is due to their low investment costs, low energy requirements, simple curing cycles, ecological convenience, good moldability, and because it is easy to encapsulate extraneous inserts, such as metal ribs and stiffeners. From the industrial viewpoint, it would be desirable to have a flexible tool which can exploit the good moldability properties and that can be easily adapted to fabricate composites with different characteristics, say materials, shape, and size, or in the presence of inserts.

In the technological literature (see, for instance, [1, 2, 3]) it is often mentioned that the identification of the production cycle is still more of an art than a science and is developed every time on a trial and error basis. Whatever small change is introduced, the whole pressure and temperature cycle to be applied, and the best location of the injection port and of the air vents, have to be identified again. This is, of course, costly and time consuming. It is therefore crucial to understand the complex phenomena involved and to develop mathematical models which can help in simulating the manufacturing procedure and identifying the appropriate range of parameters to be used in practice.

In the literature it can be seen that much has already been done in modeling and simulating the infiltration processes under the assumption that the solid preform does

*Received by the editors February 2, 1998; accepted for publication (in revised form) September 13, 1999; published electronically June 27, 2000. This research was supported by the Italian GNFM-CNR (CNR contract 98.01024.CT01 on Modelling and Simulation of Multicomponent Systems).
http://www.siam.org/journals/siap/61-1/33367.html
†Dipartimento di Matematica, Politecnico, Corso Duca degli Abruzzi 24, Torino 10129, Italy (ambrosi@calvino.polito.it, preziosi@polito.it).

not move. However, several papers show or qualitatively describe deformation of the solid preform [4, 5, 6, 7, 8, 9, 10, 11, 12, 13, 14, 15, 16, 17, 18, 19] (see also [20] for a recent review of the subject).

In fact, in several practical situations the pressure gradient driving the flow is sufficiently high enough to generate nonnegligible deformation, especially near the advancing infiltration front. This is also evident near the injection port, where a fiber-free region may appear. Actually, in some cases the resin finds it easier to deform the solid preform and to flow around it rather than through it. At the same time, the flow of the resin penetrating the preform is influenced by its compression which decreases the permeability of the porous medium to be filled up. Moreover, deformations should be taken into account when simulating composite material manufacturing in order to quantify in advance possible inhomogeneities of the final product and predict possible damages in the reinforcing network which may lead to material failure. This can be done by monitoring the deformation and stress states.

In two previous papers [21] and [22], the authors began studying the problem described above. In particular, in [21] it was assumed that the dry preform does not move during infiltration; on the contrary in [22] the coupled flow/deformation problems in the two regions (both the wet and the dry one) was studied under the assumption that in both regions the same elastic constitutive relation is valid. This allowed us to treat the interface numerically as a marker dividing the two regions which were then characterized by different material parameters. Billi and Farina [23] then proved the existence and uniqueness of a solution in self-similar form when the flow is generated by a constant pressure gradient and inertia is neglected.

This paper deduces a model aimed at simulating injection molding processes, such as resin transfer molding (RTM), structural resin injection molding (SRIM), and squeeze casting, under isothermal conditions, dropping the usual assumption that the solid preform does not deform during infiltration. In particular, the dry and wet portions of the preform are assumed to behave, respectively, elastically and inelastically in agreement with some experimental results [7, 12] and with the general observation that during infiltration the solid and the liquid constituents cannot deform independently but have to carry the load by joint deformation.

The paper is organized as follows. This introduction is followed by the second section, presenting the three-dimensional isothermal model based on the theory of deformable porous media suitable to simulate injection molding processes in those cases in which deformation of the solid preform cannot be neglected and needs to be monitored. In the third section the one-dimensional problem is formulated, while in the fourth section the boundary conditions are supplemented, together with the evolution equations of the boundaries delimiting the time-varying domains. Finally, the fifth section deals with the numerical method and discusses the results of some tests of infiltration processes in an initially dry preform.

The simulations presented show how the model can provide a description of the evolution of the deformation and stress state. This knowledge can be helpful to foresee the inhomogeneous characteristics of the material and to evaluate the possibility of damage in the reinforcing network, while identifying the range of the parameters that can be used in the production cycle.

2. The theory of deformable porous materials. Injection molding processes are some of the most commonly used methods for fabricating composites. They essentially consist of pushing a liquid melt into a porous preform. In order to model and simulate these processes, the proper theoretical framework is the theory of deformable

porous media, which can be obtained on the basis of either mixture theory or of other averaging methods, such as ensemble averages [20].

The infiltration in a deformable preform can then be described as follows. At the beginning the solid preform is dry, and therefore air fills the space within the reinforcing network. As infiltration starts, there is the formation of two time-varying domains, a dry region $\mathcal{D}^d(t)$ and a wet region $\mathcal{D}^w(t)$. We will assume saturation in $\mathcal{D}^w(t)$ so that also in each point of this region only two constituents are copresent, the solid and the resin. This corresponds to assuming that a sharp interface divides the two domains and, in particular, that no gas is trapped in the wet preform.

Assuming that the constituents of the mixture are incompressible, in the isothermal case and in absence of chemical reactions and phase changes, the coupled flow/deformation problem in the wet region $\mathcal{D}^w(t)$ can then be described by (see [20, 21, 22, 23] for further details)

$$\frac{\partial \phi_s^w}{\partial t} + \nabla \cdot (\phi_s^w \mathbf{v}_s^w) = 0 \ , \tag{2.1}$$

$$\nabla \cdot \mathbf{v}_c^w = 0 \ , \tag{2.2}$$

$$\rho_\ell \phi_\ell^w \left(\frac{\partial \mathbf{v}_\ell^w}{\partial t} + \mathbf{v}_\ell^w \cdot \nabla \mathbf{v}_\ell^w \right) = \nabla \cdot \widetilde{\mathbb{T}}_\ell^w + \mathbf{m}^w \ , \tag{2.3}$$

$$\rho_m^w \left(\frac{\partial \mathbf{v}_m^w}{\partial t} + \mathbf{v}_m^w \cdot \nabla \mathbf{v}_m^w \right) = -\nabla P_\ell^w + \nabla \cdot \mathbb{T}_m^w \ , \tag{2.4}$$

where the superscript w stands for *wet* and

- ϕ_s^w and ϕ_ℓ^w are, respectively, the volume fraction of the solid and the liquid constituents, i.e., the volume occupied by the constituent over the total volume. Saturation implies $\phi_s^w + \phi_\ell^w = 1$.
- ρ_ℓ is the density of the liquid matrix to be injected and ρ_m^w the density of the mixture as a whole, i.e.,

  $$\rho_m^w = \rho_s \phi_s^w + \rho_\ell \phi_\ell^w \ , \tag{2.5}$$

  where ρ_s is the density of the solid constituent used to fabricate the preform.
- $\mathbf{v}_\ell^w$ is the velocity of the liquid constituent, while $\mathbf{v}_m^w$ is the velocity of the mixture considered as a whole, i.e.,

  $$\mathbf{v}_m^w = \frac{\rho_s \phi_s^w \mathbf{v}_s^w + \rho_\ell \phi_\ell^w \mathbf{v}_\ell^w}{\rho_m^w} \ , \tag{2.6}$$

  where $\mathbf{v}_s^w$ is the velocity of the solid constituent. The divergence-free velocity field

  $$\mathbf{v}_c^w = \phi_s^w \mathbf{v}_s^w + \phi_\ell^w \mathbf{v}_\ell^w \tag{2.7}$$

  is a volume average velocity usually called the *composite velocity*.
- $\widetilde{\mathbb{T}}_\ell^w$ is the so-called partial stress tensor, related to the liquid constituent when the solid constituent is copresent, while $\mathbb{T}_m^w$ is the excess stress tensor related to the mixture considered as a whole; we will refer to the mixture of the solid and liquid constituents as the *wet* preform.
- P_ℓ^w is the pore liquid pressure.
- $\mathbf{m}^w$ is the so-called internal body force, which describes the microscopic interactions between the solid preform and the liquid matrix across the interface separating them.

Equation (2.1) is the mass conservation equation for the solid constituent, (2.2) is the sum of (2.1) and the mass conservation equation for the liquid constituent, (2.3) is the momentum equation for the liquid constituent, and (2.4) the one for the mixture as a whole. In (2.3)–(2.4) gravity has been neglected, but can be easily included.

The main difficulty in using (2.1)–(2.4) consists in formulating and validating the constitutive relations for the partial stress tensor for the liquid and the internal body force appearing in (2.3). In fact, $\widetilde{\mathbb{T}}_\ell^w$ refers to the single constituent when impregnating the solid, i.e., referring to the framework of mixture theory, when the other constituent is copresent, and $\mathbf{m}^w$ refers to a microscopic interaction between the constituents. Therefore, although information on the constitutive equations can be obtained on the basis of thermodynamic arguments classically used in continuum mechanics (see, for instance, the recent volume by Rajagopal and Tao [24]), these models cannot be tested directly, but only through secondary effects.

One way to overcome this difficulty is to observe, as done for instance in [25], that under some assumptions, such as the negligibility of liquid inertia, it is possible to recover from (2.3) Darcy's law

$$\mathbf{v}_\ell^w - \mathbf{v}_s^w = -\frac{\mathbb{K}(\mathbb{F}_s^w)}{\mu\phi_\ell^w}\nabla P_\ell^w \ , \tag{2.8}$$

where $\mathbb{K}$ is the permeability tensor, $\mathbb{F}_s^w$ is the deformation gradient related to the solid constituent, and μ is the liquid viscosity. Darcy's law is known to be applicable with confidence to the class of problems considered in the present paper and is then used to replace (2.3). Several generalizations of Darcy's law could be considered here, e.g., the Forchheimer law or corrections to take into account the non-Newtonian properties of the resin. However, in the present work we will assume the validity of Darcy's law in the form (2.8).

After the assumptions above, the only quantity which is still constitutively to be specified is the stress tensors $\mathbb{T}_m^w$, which refers to the behavior of the mixture considered as a whole. This information can be both obtained using classical continuum mechanics tools and validated directly by conceiving of suitable but standard experiments, e.g., steady compression tests, oscillatory twist and compression, and creep and stress relaxation tests to be performed on the wet preform.

Unfortunately, to our knowledge there are only two papers [7, 12] describing from the experimental viewpoint the viscoelastic behavior of wet and dry preforms. Kim, McCarthy, and Fanucci [7] performed some experiments addressed at the study of the stress relaxation properties of a wet preform finding a spectrum of relaxation times. They also point out the different behavior of wet and dry preforms subject to static compression. Nam et al. [12] investigated creep deformation of a commercial prepreg, measuring a retardation time of the order of 200 seconds. In addition, several other authors [5, 10, 15, 16, 20, 26] have reported viscoelastic behaviors of the materials they use with nonnegligible relaxation or retardation times. However, we mention that depending on the microscopic structure of the preform, plastic phenomena can also be present. This can result, for instance, because of the displacement of single fibers in the reinforcements.

On the basis of these observations, and on the fact that the solid preform and the liquid matrix cannot deform independently but have to carry the load by joint deformation, we will model the wet preform as an inelastic solid, corresponding to the following constitutive equation:

$$\lambda\frac{\mathcal{D}\mathbb{T}_m^w}{\mathcal{D}t} + \mathbb{T}_m^w = \Lambda\frac{\mathcal{D}\mathbb{G}_m(\mathbb{E}_s^w)}{\mathcal{D}t} + \mathbb{G}_m(\mathbb{E}_s^w) \ , \tag{2.9}$$

where λ is the relaxation time, Λ is the retardation time, $\Lambda \geq \lambda$, $\mathbb{E}_s^w$ is the Lagrangian strain tensor, $\mathcal{D}/\mathcal{D}t$ is a frame invariant convective derivative, and $\mathbb{G}_m$ is a tensorial function of the Lagrangian strain tensor.

In particular, for numerical purposes it is convenient to introduce the new variable

$$\mathbb{S}_m = \lambda \mathbb{T}_m^w - \Lambda \mathbb{G}_m(\mathbb{E}_s^w) \ , \tag{2.10}$$

which allows us to rewrite the inelastic constitutive equation (2.9) as

$$\lambda \frac{\mathcal{D}\mathbb{S}_m}{\mathcal{D}t} + \mathbb{S}_m = (\lambda - \Lambda)\mathbb{G}_m(\mathbb{E}_s^w) \ . \tag{2.11}$$

Equation (2.11) says that, for given $\mathbb{G}_m$, in an interval of time of the order of λ the quantity $\mathbb{S}_m$ will reach its equilibrium value $\mathbb{S}_m = (\lambda - \Lambda)\mathbb{G}_m$, i.e., $\mathbb{T}_m^w = \mathbb{G}_m(\mathbb{E}_s^w)$. Furthermore, it can be noticed that when $\lambda = \Lambda$, (2.11) is satisfied, for suitable initial conditions, by $\mathbb{S}_m = 0$; that is, the wet porous material behaves elastically.

One can then write the following model in the wet region:

$$\begin{cases} \dfrac{\partial \phi_s^w}{\partial t} + \nabla \cdot (\phi_s^w \mathbf{v}_s^w) = 0 \ , \\ \nabla \cdot \left[\mathbf{v}_s^w - \dfrac{\mathbb{K}}{\mu} \nabla P_\ell^w \right] = 0 \\ \rho_s \phi_s^w \left(\dfrac{\partial \mathbf{v}_s^w}{\partial t} + \mathbf{v}_s^w \cdot \nabla \mathbf{v}_s^w \right) = -\nabla P_\ell^w + \nabla \cdot \mathbb{T}_m^w \\ \lambda \dfrac{\mathcal{D}\mathbb{S}_m}{\mathcal{D}t} + \mathbb{S}_m = (\lambda - \Lambda)\mathbb{G}_m(\mathbb{E}_s^w) \ , \end{cases} \quad \text{in } \mathcal{D}^w(t), \tag{2.12}$$

and

$$\mathbf{v}_\ell^w = \mathbf{v}_s^w - \frac{\mathbb{K}(\mathbb{F}_s^w)}{\mu(1-\phi_s^w)} \nabla P_\ell^w \ . \tag{2.13}$$

$\mathbb{T}_m^w, \mathbb{S}_m, \mathbb{G}_m$ are related through (2.10).

As far as the dry region is concerned, (2.1)–(2.4) can be rewritten with obvious changes, that is, the superscript w with d, standing for *dry*, and considering air as the impregnating fluid. However, the viscosity of air is so small, and therefore is so easily expelled from the dry preform offering negligible resistance that its contribution to the excess stress of the mixture $\mathbb{T}_m^d$ can be neglected and it reduces to $\mathbb{T}_s^d$. Coherently, the pore pressure is assumed constant in the dry material. In addition, air density is so small that its contribution to the inertial term is again negligible. Hence, (2.4) rewrites as an equation involving the solid constituent only, without any interaction term with the gas. Mass and momentum balance (2.2)–(2.3) for the gas can then be neglected.

Assuming that the dry preform behaves elastically

$$\mathbb{T}_s^d = \mathbb{G}_s(\mathbb{E}_s^d) \ , \tag{2.14}$$

we can then write the following model in the dry region:

$$\begin{cases} \dfrac{\partial \phi_s^d}{\partial t} + \nabla \cdot (\phi_s^d \mathbf{v}_s^d) = 0 \\ \rho_s \phi_s^d \left(\dfrac{\partial \mathbf{v}_s^d}{\partial t} + \mathbf{v}_s^d \cdot \nabla \mathbf{v}_s^d \right) = \nabla \cdot \mathbb{G}_s \end{cases} \quad \text{in } \mathcal{D}^d(t). \tag{2.15}$$

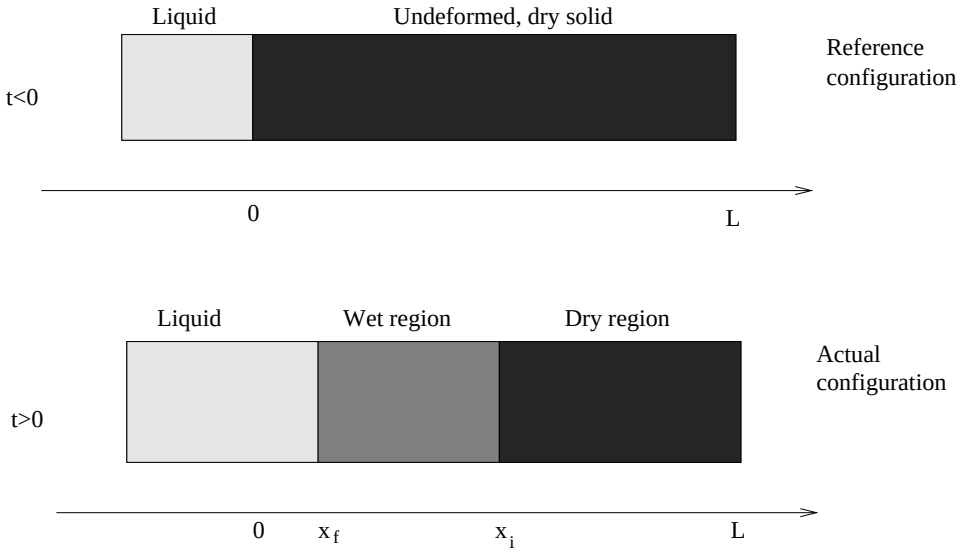

FIG. 1. *One-dimensional infiltration problem.*

In order to close the problem one should join to (2.12) and (2.15) proper boundary conditions. However, there are several questions on this topic still not well understood, such as the generalization of the Beavers–Joseph condition to the deformable case or the fact that boundary conditions should be based on surface area fractions which might not be equal to volume fractions [20, 28, 29, 30]. From now on we deal with one-dimensional problems and omit further details.

3. The one-dimensional case. Consider now a one-dimensional infiltration problem along a principal direction of the preform permeability tensor, and, referring to Figure 1, denote by $x_f(t)$ the left border of the preform and by $x_i(t)$ the infiltration front. The identification of a sharp infiltration front can be done if capillarity phenomena are negligible; this is possible in composite manufacturing processes, since in most cases the capillary pressures are much smaller than the applied infiltration pressures. A fully draining boundary constrains the right border of the solid preform to be fixed at $x = L$, but allows, at the same time, both air and liquid matrices to pass through with no drag.

For $t \leq 0$ the whole preform is dry, at rest, and compressed at a given volume ratio $\phi_0(x)$, i.e.,

$$\begin{cases} \phi_s^d(x, t = 0) = \phi_0(x) & \text{for } x \in [0, L]; \\ \\ x_f(t = 0) = x_i(t = 0) = 0 \ . \end{cases}$$

Usually, $\phi_s^d(x, t = 0) = \phi_r$, where ϕ_r corresponds to the undeformed configuration.

The flow of the liquid matrix is in the positive direction. Time $t = 0$ is chosen as the instant in which the liquid touches the left border of the preform. The incoming liquid then compresses the sponge while the fluid starts infiltrating. Therefore, while the right border of the sponge stays fixed at $x = L$, the other one moves to $x = x_f(t)$, and part of the preform, precisely up to $x = x_i(t)$, wets up. One can then identify a wet region $\mathcal{D}^w(t) = [x_f(t), x_i(t)]$ and a dry region $\mathcal{D}^d(t) = [x_i(t), L]$ divided by the infiltration front $x_i(t)$, which is an interface moving with the liquid.

As infiltration proceeds both the dry and wet preforms compress or expand, according to the flow conditions, and therefore both x_f and x_i depend on time.

Before proceeding, it is useful to observe that, in one-dimensional problems, (2.2) and the similar equation in the dry region can be rewritten

$$\frac{\partial v_c^w}{\partial x} = \frac{\partial v_c^d}{\partial x} = 0 \ , \tag{3.1}$$

which implies that the composite velocity is space-independent in each subdomain:

$$v_c(x,t) = \begin{cases} v_c^w(t) & \text{in } \mathcal{D}^w(t)\,; \\ \\ v_c^d(t) & \text{in } \mathcal{D}^d(t)\,. \end{cases} \tag{3.2}$$

In the following section we will show that the composite velocity must be continuous across both material interfaces $x_f(t)$ and $x_i(t)$; therefore the composite velocity has to be constantly equal to the inflow velocity

$$v_c(x,t) = u_{in}(t) \tag{3.3}$$

in all the domain. This allows us to write, recalling (2.8),

$$v_s = u_{in} + \frac{K(\phi_s^w)}{\mu}\,\frac{\partial P_\ell^w}{\partial x} \ , \tag{3.4}$$

$$v_\ell = u_{in} - \frac{\phi_s^w}{1-\phi_s^w}\,\frac{K(\phi_s^w)}{\mu}\,\frac{\partial P_\ell^w}{\partial x}, \tag{3.5}$$

where we have used the property that in one-dimensional problems strain and volume ratio are one-to-one related. In particular, (3.4) can be used to eliminate the pressure so that (2.12) and (2.15) give rise to the following one-dimensional model:

(3.6)

$$\begin{cases} \dfrac{\partial \phi_s^w}{\partial t} + v_s^w \dfrac{\partial \phi_s^w}{\partial x} + \phi_s^w \dfrac{\partial v_s^w}{\partial x} = 0 \ , \\ \rho_s \phi_s^w \left(\dfrac{\partial v_s^w}{\partial t} + v_s^w \dfrac{\partial v_s^w}{\partial x} \right) + \dfrac{\mu}{K(\phi_s^w)} [v_s^w - u_{in}(t)] + \dfrac{\partial T_m}{\partial x} = 0, \\ \dfrac{\partial S_m}{\partial t} + v_s^w \dfrac{\partial S_m^w}{\partial x} + \dfrac{S_m}{\lambda} + \left(\dfrac{\Lambda}{\lambda} - 1 \right) G_m(\phi_s^w) = 0 \text{ in } \ \mathcal{D}^w = [x_f(t), x_i(t)], \end{cases}$$

(3.7)

$$\begin{cases} \dfrac{\partial \phi_s^d}{\partial t} + v_s^d \dfrac{\partial \phi_s^d}{\partial x} + \phi_s^d \dfrac{\partial v_s^d}{\partial x} = 0 \\ \\ \rho_s \phi_s^d \left(\dfrac{\partial v_s^d}{\partial t} + v_s^d \dfrac{\partial v_s^d}{\partial x} \right) + G'_s(\phi_s^d) \dfrac{\partial \phi_s^d}{\partial x} = 0 \end{cases} \qquad \text{in } \ \mathcal{D}^d = [x_i(t), L],$$

where

$$S_m = -(\mathbb{S}_m)_{xx}, \qquad T_m = -(\mathbb{T}_m^w)_{xx} = \frac{S_m}{\lambda} + \frac{\Lambda}{\lambda} G_m(\phi_s^w) \ , \tag{3.8}$$

and $G_m = -(\mathbb{G}_m)_{xx}$ and $G_s = -(\mathbb{G}_m)_{xx}$ are strictly increasing functions of the volume ratio:

$$G'_s = \frac{dG_s}{d\phi_s^d} > 0 \ , \qquad G'_m = \frac{dG_m}{d\phi_s^w} > 0 \ . \tag{3.9}$$

In writing (3.6)–(3.9) we have used the common convention adopted in most papers dealing with one-dimensional problems for deformable porous media: the stress is considered (and measured) as positive in compression.

A characteristic analysis of the system of equations (3.6)–(3.7) shows that the equations driving the flow in the dry region are always hyperbolic. Conversely, the nature of the equations driving the flow in the wet region (3.6) is hyperbolic if $\frac{\partial T_m}{\partial \phi_s^w} > 0$ for any ϕ_s^w in the range of the application. In fact the eigenvalues of the Jacobian associated with problem (3.6) are

$$c^{\pm} = v_s \pm \sqrt{\frac{1}{\rho_s}\frac{\partial T_m}{\partial \phi_s^w}}, \qquad c^0 = v_s \ , \tag{3.10}$$

where T_m depends on S_m and G_m as given by the relationship (3.8), where it should be kept in mind that $G_m = G_m(\phi_s^w)$ as well as S_m satisfies the last equation in (3.6). Although G'_m is always a positive quantity, it is not ensured in principle that $\frac{\partial T_m}{\partial \phi_s^w}$ is positive, so that eigenvalues with a complex part may appear. In such a case the equations show locally a partially elliptic behavior.

It should be noticed that in (3.6) we chose the covariant convective derivative of S_m, based on the velocity of the solid for analogy with the momentum equation. The question of which convective derivative should be used to have the best comparison with experiments is still open and already addressed in [21].

The quantity $u_{in}(t)$ which appears in (3.3)–(3.6) depends on which physical quantity is controlled during the infiltration: the flow can be *velocity driven* (control of the velocity at the inflow) or *pressure driven* (control of the inflow pressure). In the simulations to follow we shall assume that the liquid is pushed at a given velocity, say constant.

The analysis of (3.6) reveals that four typical time scales (respectively, velocities) of the problem can be identified. The first one is the time which is necessary for an acoustic wave, traveling at speed $c^{\pm}$, to go through the whole porous preform. The second typical time of the problem is related to the attenuation of the acoustic waves due to dissipative phenomena, which stem from the nature of Darcy's law. The third is the time necessary to infiltrate the whole preform, which is related to the velocity of the injected liquid u_{in}. This is usually much longer than the previous times, so that a very small portion of the preform is wet when the waves due to initial conditions are damped out. The last typical time is the relaxation time λ; its value is usually larger (even an order of magnitude larger) than the time needed to infiltrate the preform. Another characteristic time $\Lambda > \lambda$ appears in (3.6), which is usually of the order of λ. As the time scales discussed above are usually very different, the infiltration of a liquid into an anelastic porous preform with nonnegligible inertia can be said to belong to the class of *stiff* problems.

In this respect, we can observe that inertial terms are to be necessarily retained to obtain a realistic description of the early instances of the infiltration process. In such an interval of time, the preform rapidly compresses, starting from rest, so that the stresses in the preform adjust to the pressure applied to generate infiltration. After

the very early stages of infiltration, inertial terms could be dropped. This would bring a change of type in the system of partial differential equations as hyperbolicity would be lost: the momentum equation would be written as a stress equilibrium equation, without time derivatives. This assumption would partially smooth the stiffness of the problem (the time scale related to inertia is lost) but an approximation of the dynamics of the infiltration at early times is introduced.

These considerations can be simply highlighted in the case of flow driven by a constant pressure ΔP. If inertia is neglected, a sudden compression of the dry preform is generated as soon as the extremum x_f is in touch with the liquid, as the momentum equation is written as a stress balance equation and therefore the preform has to compress to balance the applied pressure. This gives rise to an infinite initial velocity of propagation of the free border x_f which suddenly moves to the position

$$x_f(t=0) = L\left(1 - \frac{\phi_0}{\phi_0^+}\right),$$

where $G_s(\phi_0^+) = \Delta P$, so that the stress in the dry region is equal to the pressure difference (stress balance).

4. Interface and boundary conditions. In order to close the problem, we still have to add proper interface and boundary conditions for (3.6)–(3.7). The interface $x_i(t)$ and the free boundary $x_f(t)$ are material interfaces fixed on the liquid constituent and on the solid constituent, respectively, and therefore

$$\frac{dx_i}{dt} = v_\ell^w(x_i(t), t)\ , \tag{4.1}$$

$$\frac{dx_f}{dt} = v_s^w(x_f(t), t)\ . \tag{4.2}$$

Boundary and interface conditions for a mixture are a very delicate issue and still a matter of debate. Controversies involve, for instance,

- the splitting of the stress and interface conditions in traction problems [24, 36];
- the validity of the Beavers–Joseph boundary condition [37, 38], its generalization to deformable porous media and to impinging flows;
- the slip condition at the mold wall;
- the difference between volume fraction and surface area fraction. Several methods can be used to deduce boundary conditions, e.g., continuity of chemical potential, the notion of saturation, diffusing singular surfaces, homogenization methods, and can lead to slightly different results [24, 37].

Controversies essentially stem from the intrinsic difficulty in stating boundary conditions relating regions where equations for average quantities are postulated (where the *average* is to be defined in an appropriate sense).

Following [31] and [32], we assume that the equations for the whole mixture must provide the correct boundary conditions. When writing the integral form of (3.6) and (3.7) one finds the following jump conditions:

$$[\![\rho_m(v_m - v_\sigma)]\!] = 0, \tag{4.3}$$

$$[\![T_m + \rho_s\phi_s v_s(v_s - v_\sigma)]\!] = 0\,, \tag{4.4}$$

where v_σ is the velocity of the interface. The continuity of the pore pressure is implicit in (4.4) and can be related either to the continuity of chemical potential [31] (more

precisely from postulating null jump of energy, entropy, and temperature) or to the assumption of validity of Darcy's law. This is due to the fact that the pressure gradient appearing in the mixture equation actually acts as a bulk dissipative force.

We remark that both the momentum equations in (3.6) and (4.4) involve the stress tensor of the *mixture* and that the constituents of the mixture are incompressible.

If $v_\sigma = v_s$, then one can write

$$\rho_m(v_m - v_s) = \rho_\ell \phi_\ell (v_\ell - v_s) = \rho_\ell (v_c - v_s)\,, \tag{4.5a}$$

while if $v_\sigma = v_\ell$,

$$\rho_m(v_m - v_\ell) = \rho_s \phi_s (v_s - v_\ell) = \rho_s (v_c - v_\ell)\,. \tag{4.5b}$$

Specializing then (4.3)–(4.4) to $x_f(t)$, which is a material surface fixed on the solid ($v_\sigma = v_s$), one has

$$v_c^w = u_{in} \qquad \text{on } x_f(t). \tag{4.6}$$

$$T_m = 0 \tag{4.7}$$

Equation (4.6) states the continuity of v_c across $x_f(t)$. In the same way one can prove the continuity of v_c also on $x_i(t)$. Hence, recalling (3.2) v_c is everywhere equal to the inflow velocity $u_{in}(t)$.

Specializing (4.3)–(4.4) to the interface $x_i(t)$ ($v_\sigma = v_l$), which is a material surface fixed on the liquid, one has

$$\phi_s^d (v_s^d - v_\ell) = \phi_s^w (v_s^w - v_\ell) \qquad \text{on } x_i(t). \tag{4.8}$$

$$G_s(\phi_s^d) + \rho_s \phi_s^d v_s^d (v_s^d - v_\ell) = T_m + \rho_s \phi_s^w v_s^w (v_s^w - v_\ell) \tag{4.9}$$

In addition, the constitutive equation in (3.6) calls for another boundary condition when the characteristics related to the convective velocity v_s enter the infiltrated domain. The border $x_f(t)$ is fixed on the solid and therefore in the (x,t) space it moves along a characteristic line, and then no boundary condition has to be given on it. Conversely, the infiltration front is wetting the solid more and more, i.e., $v_\ell > v_s$, and one interface condition has to be given.

In order to understand what condition should be given, we will reason step-by-step as follows, being aware that the position of the boundary conditions in this class of problems is still an open question in the literature. If the wet preform behaves elastically, no extra conditions are needed, as the infiltration front (4.6)–(4.9) is sufficient for the problem to be well formulated.

Under the very particular assumption that the wet and dry porous materials behave elastically and, in the same way, that is, if $\lambda = \Lambda$ and $G_m = G_s$, (4.6)–(4.9) imply continuity of volume ratio and of velocity of the solid constituent through $x_i(t)$. On the other hand, if $\lambda = \Lambda$ and $G_m \neq G_s$, i.e., the wet and the dry porous materials behave elastically but according to different stress–strain relationships, then continuity of volume ratio does not hold any more and one has to deal with state variables which are not continuous across the interface separating the two domains.

The reason for the discontinuity can be easily understood neglecting inertial terms, which are very small when assuming that the infiltration process is already

at an advanced stage. In this case, if different stress–strain relations are valid in the two regions, then two different volume ratios are necessary on the two sides of the interface to satisfy the continuity of stress across the interface. Now, in order to have a continuous composite velocity, since the liquid velocity is equal to the interface velocity on both sides, the velocity of the solid constituent has to adjust properly and, in particular, in a discontinuous fashion.

In particular, this means that if one focuses on what happens in the region around a material point of the dry region when it is crossed by the infiltration front, one can see that when dry the preform is compressed at a volume ratio $\hat{\phi}$ corresponding to a stress $T_s = G_s(\hat{\phi})$. When it is crossed by the infiltration front, because of the continuity of the stress across x_i, the value of the stress in the material point under consideration is still $T_m = T_s = G_s(\hat{\phi})$, but since $G_m < G_s$, the preform suddenly compresses to a higher volume ratio $\phi_s^w = G_m^{-1}(G_s(\hat{\phi})) > \hat{\phi}$. This immediate response is a typical characteristic of elastic materials and is shown in Figure 7.

If, instead, the wet preform exhibits creep behavior (as in Voigt–Kelvin or standard linear solids), then the volume ratio in the point crossed by the interface takes some time to reach the value corresponding to the elastic case. Following this argument, it is expected that not only the stress, but also the volume ratio, shall be continuous across the infiltration front:

$$\phi_s^w(x_i(t),t) = \phi_s^d(x_i(t),t) \ , \tag{4.10}$$

which in turn implies the continuity of v_s and

$$T_m(x_i(t),t) = G_s(\phi_s^d(x_i(t),t)) \ , \tag{4.11}$$

corresponding to continuity of the stress tensor of the mixture which, in terms of S_m, becomes

$$S_m(x_i(t),t) = \lambda G_s(x_i(t),t) - \Lambda G_m(x_i(t),t) \ . \tag{4.12}$$

Summing up, the boundary and interface conditions are

$$\begin{cases} S_m(x_f(t),t) = -\Lambda G_m(x_f(t),t), \\ S_m(x_i(t),t) = \lambda G_s(x_i(t),t) - \Lambda G_m(x_i(t),t) \ , \\ \phi_s^w(x_i(t),t) = \phi_s^d(x_i(t),t), \\ v_s^w(x_i(t),t) = v_s^d(x_i(t),t) \ , \\ v_s^d(L,t) = 0 \ , \end{cases} \tag{4.13}$$

and the evolution equation for the interfaces are

$$\begin{cases} \dfrac{dx_f}{dt} = v_s^w(x_f(t),t), \\ \\ \dfrac{dx_i}{dt} = \dfrac{u_{in}(t) - \phi_s^w(x_i(t),t) v_s^w(x_i(t),t)}{1 - \phi_s^w(x_i(t),t)} \ . \end{cases} \tag{4.14}$$

When the solid preform is fully infiltrated, i.e., $\mathcal{D}^d = \emptyset$, then the integration of the initial boundary value problem involves only (3.6) with the evolution equation (4.2), and the boundary conditions

$$T_m(x_f(t),t) = 0 \qquad \text{and} \qquad v_s^w(L,t) = 0 \ . \tag{4.15}$$

5. Simulation and results. In this section the numerical approximation of the system of equations (3.6)–(3.7), with the evolution equations (4.14), and the boundary and interface conditions (4.13) is addressed. In the following we focus on the discretization of the equations governing the flow in the wet regions, as the equations driving the flow in the dry region are much the same except for a few missing terms. To allow for a more general analysis of the numerical results, it proves useful to rewrite part of (3.6)–(3.7) in conservation form using nondimensional variables.

In order to do that, we introduce the mass fluxes $q_s^w = \phi_s^w v_s^w$ and $q_s^d = \phi_s^d v_s^d$ and denote

$$K_r = K(\phi_r^d) \qquad \text{and} \qquad G_r' = \frac{dG_s(\phi_r^d)}{d\phi_s}, \tag{5.1}$$

where ϕ_r^d is such that $G_s(\phi_r^d) = 0$.

The dimensionless variables are, then, obtained by scaling lengths with the initial length of the preform L, velocities with a characteristic velocity U, time with L/U, stresses with G_r', and S_m with $(\Lambda - \lambda)G_r'$. Taking $\hat{u}_{in}$ as the reference velocity, the dimensionless system of equations then reads

$$\frac{\partial \phi_s^w}{\partial t} + \frac{\partial q_s^w}{\partial x} = 0 \ , \tag{5.2}$$

$$\mathcal{P}\frac{\partial q_s^w}{\partial t} + \frac{\partial}{\partial x}\left[\mathcal{P}\frac{(q_s^w)^2}{\phi_s^w} - \mathcal{Q}T_m\right] = \frac{1}{\widetilde{K}(\phi_s^w)}\left[\widetilde{u}_{in}(t) - \frac{q_s^w}{\phi_s^w}\right] \ , \tag{5.3}$$

$$\mathcal{R}\left(\frac{\partial S_m}{\partial t} + v_s^w \frac{\partial S_m}{\partial x}\right) + S_m + \widetilde{G}_m(\phi_s^w) = 0 \tag{5.4}$$

with

$$T_m = (\mathcal{L} - 1)\, S_m + \mathcal{L}\widetilde{G}_m(\phi_s^w) \ , \tag{5.5}$$

and where from now on all quantities are nondimensional, and, in particular,

$$\widetilde{K}(\phi_s^w) = \frac{K(\phi_s^w)}{K_r} \ , \qquad \widetilde{G}_m(\phi_s^w) = \frac{G_m(\phi_s^w)}{G_r'} \ , \qquad \widetilde{G}_s(\phi_s^d) = \frac{G_s(\phi_s^d)}{G_r'} \ . \tag{5.6}$$

The coupled flow/deformation problem (5.2)–(5.4) depends on the four dimensionless parameters

$$\mathcal{L} = \frac{\Lambda}{\lambda}, \qquad \mathcal{P} = \frac{\rho_s \hat{u}_{in} K_r}{\mu L} \ , \qquad \mathcal{Q} = \frac{G_r' K_r}{\mu \hat{u}_{in} L} \ , \qquad \mathcal{R} = \frac{\lambda \hat{u}_{in}}{L} \ . \tag{5.7}$$

The parameter $\mathcal{L}$ is the ratio between retardation and relaxation times appearing in the stress constitutive equation. $\mathcal{P}$ accounts for the relevance of the inertial terms with respect to the pressure gradient (appearing through the Darcy law). $\mathcal{Q}$ represents the ratio between fluid pressure and excess stress while $\mathcal{R}$ is the ratio between relaxation time and the time that would be needed by the fluid to travel the relaxed preform length at the constant inflow velocity.

The remaining equations and initial, interface, and boundary conditions remain formally unchanged.

The choice of a proper numerical discretization of the system (5.2)–(5.4) depends on its mathematical nature. As discussed in a previous section, the system of equations driving the flow in the dry region is hyperbolic. The mathematical type of the

system driving the flow in the wet region (5.2)–(5.4) depends on the sign of $\frac{\partial T_m}{\partial \phi_s^w}$: it is hyperbolic if $\frac{\partial T_m}{\partial \phi_s^w}$ is always positive, but it has locally an imaginary part of the eigenvalues (and then elliptic behavior), where $\frac{\partial T_m}{\partial \phi_s^w} < 0$.

As the hyperbolic character of the equations in a typical simulation is dominant also in the wet part, the numerical scheme is designed in both subdomains using a hyperbolic decomposition of the equations. Equations (5.2), (5.3) can be written in vectorial form as

$$\frac{\partial \mathbf{u}}{\partial t} + \frac{\partial \mathbf{f}}{\partial x} = \mathbf{s}(\mathbf{u}) \ , \tag{5.8}$$

where

$$\mathbf{u} = (\phi, \mathcal{P}q), \tag{5.9}$$

and

$$\mathbf{f} = \left(q, \mathcal{P}\frac{q^2}{\phi} + \mathcal{Q}T_m \right), \tag{5.10}$$

$$\mathbf{s} = \left(0, \frac{1}{\widetilde{K}(\phi)} \left(u_{in}(t) - \frac{q}{\phi} \right) \right). \tag{5.11}$$

For numerical purposes, as the integration domain stretches in time, it is useful to consider the integral formulation of the equation above, because at a discrete level it allows us to easily take into account the movements of the grid nodes. The integral formulation of the conservation law (5.8) reads [30, 31]

$$\frac{d}{dt} \int_{x_1(t)}^{x_2(t)} \mathbf{u} \ dx + \mathbf{f}(x_2(t)) - \mathbf{f}(x_1(t)) = \int_{x_1(t)}^{x_2(t)} \mathbf{s}(\mathbf{u}) \ dx \tag{5.12}$$

$$\forall (x_1(t), x_2(t)) \subseteq (x_f(t), x_i(t)),$$

where $\mathbf{u}, \mathbf{s}$ have already been defined, and $\mathbf{f}$ is defined now as

$$\mathbf{f} = \left(q - v^{'} \phi, \mathcal{P}q \left(\frac{q}{\phi} - v^{'} \right) + \mathcal{Q}T_m \right). \tag{5.13}$$

The relationship (5.13) takes into account the movement of the extrema of the interval $(x_1(t), x_2(t))$. It gives the generalized form of the flux vector when considering possibly moving domains with velocity $v'(x,t)$. The contribution of the flux involving v' in (5.13) says that the total quantity of $\mathbf{u}$ in the interval $(x_1(t), x_2(t))$ changes in time while flowing through the boundary because of the movement of the boundary itself. As the whole solid preform lies in $(x_f(t), x_i(t)) \cup (x_i(t), L)$ we divide the wet region into M equally spaced intervals with size $(\Delta x)_w^n$ and the dry region into $N - M$ equally spaced intervals with size $(\Delta x)_d^n$. The discrete solution $\mathbf{u}_i$ is defined as the integral of $\mathbf{u}(x)$ into the ith interval, as well as the $N+1$ numerical fluxes f_i, $i = 0, \ldots, N$, are defined at the border of the intervals. This allows us to impose naturally the boundary conditions on the value of the fluxes at the boundary, as discussed in the fourth section.

The movement of the material boundaries $x_f(t)$ and $x_i(t)$ requires a stretching of the computational domain. As the mechanical properties of the two subdomains are different, the numerical stretching of the wet and dry parts of the porous preform are independent; only the interface must correspond to a node of the computational grid. From a numerical point of view, it is desirable to take into account the movement of the solid, preserving at the same time a constant distance between the discretization nodes. This is accomplished by imposing a proper discrete mesh velocity movement $v_j'^n$, $j = 0, \ldots, N$, such that the discretized counterpart of (5.9) reads

$$\frac{1}{\Delta t}\left[(\Delta x)^{n+1}\mathbf{u}_j^{n+1} - (\Delta x)^n \mathbf{u}_j^n\right] + \mathbf{f}_j^n - \mathbf{f}_{j-1}^n = (\Delta x)^{n+1}\mathbf{s}(\mathbf{u}_j^{n+1}) \ , \tag{5.14}$$

where $\mathbf{f}_j^n$ depends on the solution $\mathbf{u}^n$ and on the velocity of the grid $v_j'^n$, which is defined as follows:

$$v_j'^n = (v_M'^n - v_0'^n)\frac{j}{M} + v_0'^n \ , \qquad j = 0, \ldots, M \ . \tag{5.15}$$

$$v_j'^n = v_M'^n \frac{N-j}{N-M} \ , \qquad j = M+1, \ldots, N \ , \tag{5.16}$$

where

$$v_0'^n = \frac{dx_f}{dt}(t = t^n), \qquad v_M'^n = \frac{dx_i}{dt}(t = t^n) \ . \tag{5.17}$$

In this way, the convective flux at the material boundary, i.e., $\mathbf{f}_0$, is automatically zero and, at the same time, the intervals move in such a way that they all have the same length $(\Delta x)^n$. It is to be remarked that v_j' coincides with the material velocity of the solid at the left boundary. The position of the jth point at time $n+1$ is $x_j^n + v_j'^n \Delta t$ and the spatial integration step $(\Delta x)_w^{n+1}$ is

(5.18)

$$\begin{aligned}(\Delta x)_w^{n+1} &= \left(x_j^n + v_j'^n \Delta t\right) - \left(x_{j-1}^n + v_{j-1}'^n \Delta t\right) \\ &= \left[x_j^n + \left((v_M'^n - v_0'^n)\frac{j}{M} + v_0'^n\right)\Delta t\right] - \left[x_{j-1}^n + \left((v_M'^n - v_0'^n)\frac{j-1}{M} + v_0'^n\right)\Delta t\right] \\ &= (\Delta x)_w^n + \left(v_M'^n - v_0'^n\right)\frac{\Delta t}{M} \ ,\end{aligned}$$

and analogously $(\Delta x)_d^{n+1}$. In particular, if the integration intervals are initially equispaced in each subdomain, they remain equispaced at all the time steps.

The source term on the right-hand side of (5.14) can be straightforwardly discretized implicitly, because it is not differential: when first computing ϕ^{n+1}, the implicit discretization of $\mathbf{s}^{n+1}$ can be easily performed, because $\mathbf{s}$ depends linearly on q, as may be seen in (5.11).

The proper boundary conditions to be imposed at the borders of the computational domain are that mass and convective momentum flux on both sides of the sponge must vanish; moreover, the left boundary of the sponge is stress-free, while the stress at the right boundary is unknown. Therefore, the flux vector at the free solid boundary is prescribed as follows:

$$\mathbf{f}_0^n = (0, 0)^t. \tag{5.19}$$

At the constrained solid boundary zero convective flux has to be imposed, but no specific value of the stress (which is unknown) can be prescribed. This task is accomplished numerically introducing a dummy computational cell, just out of the border, where the solution is supposed to have such a value that the flux computed through the constrained border has always a zero convective contribution:

$$\phi_{N+1}^n = \phi_N^n, \qquad q_{N+1}^n = -q_N^n. \tag{5.20}$$

The form of the discrete flux $\mathbf{f}_i^n$ and its dependence on $\mathbf{u}^n$ in the interior of the computational domain remain to be defined. We do not go into details about this but just mention that a numerical approach which is well suited for nonlinear conservation laws has been adopted. Namely, the numerical flux is computed by a second order upwind scheme, exploiting a characteristic decomposition of the Jacobian of the function $\mathbf{f}(\mathbf{u})$ (see [33, 34, 35] for the basic mathematical background). This technique avoids nonphysical oscillations in the solution, even when it has a discontinuous nature, and ensures conservation of the unknowns. When the local velocity of sound is found to be negative, the numerical flux is simply defined in a centered way as follows:

$$\mathbf{f}_j^n = \frac{1}{2}\left(\mathbf{f}(\mathbf{u}_j^n) + \mathbf{f}(\mathbf{u}_{j+1}^n)\right). \tag{5.21}$$

Equation (5.4) cannot be written in conservation form and is then discretized separately, by a simple upwind scheme, with implicit discretization of the source term:

(5.22)

$$S_i^{n+1} - S_i^n + \frac{\Delta t}{2\Delta x}\left(v_j^n - v_j^{'n}\right)\left(S_{j+1}^n - S_{j-1}^n\right) - \frac{\Delta t}{2\Delta x}|v_j^n - v_j^{'n}|\left(S_{j+1}^n - 2S_j^n + S_{j-1}^n\right) + \frac{\Delta t}{\mathcal{R}} S_j^{n+1} + \frac{\Delta t}{\mathcal{R}} G_m^w(\phi_j^{n+1}) = 0.$$

At the beginning of the simulation, the wet part of the preform is composed only of one discrete interval and the dry region is divided into $N-1$ intervals. As time goes by, the interface travels toward the dry border, the size of the spatial integration step in the dry region grows, and the size of the intervals in the wet region diminishes. It is then clear that, at a certain time, when the stretching of the initial grid has become excessive, a remeshing is necessary to preserve the initial spatial accuracy. This operation is carried out every time so that

$$|(\Delta x)^n - (\Delta x)^0| > \alpha(\Delta x)^0\ , \tag{5.23}$$

where, for example, $\alpha = 0.1$. This remeshing involves a projection of the solution from the stretched grid into a new one, the latter having a spatial size as near as possible to the original one. The projection is made in such a way to preserve the L^1 norm of the solution in each subdomain.

In order to perform the numerical simulations using a range of parameters as realistic as possible, in the computations which follow we use stress–strain relations extrapolated from the data measured by Kim, McCarthy, and Fanucci [7] for dry and lubricated fiber materials (see Figure 2),

$$G = \beta(e^{\gamma\phi} - e^{\gamma\phi_r}), \tag{5.24}$$

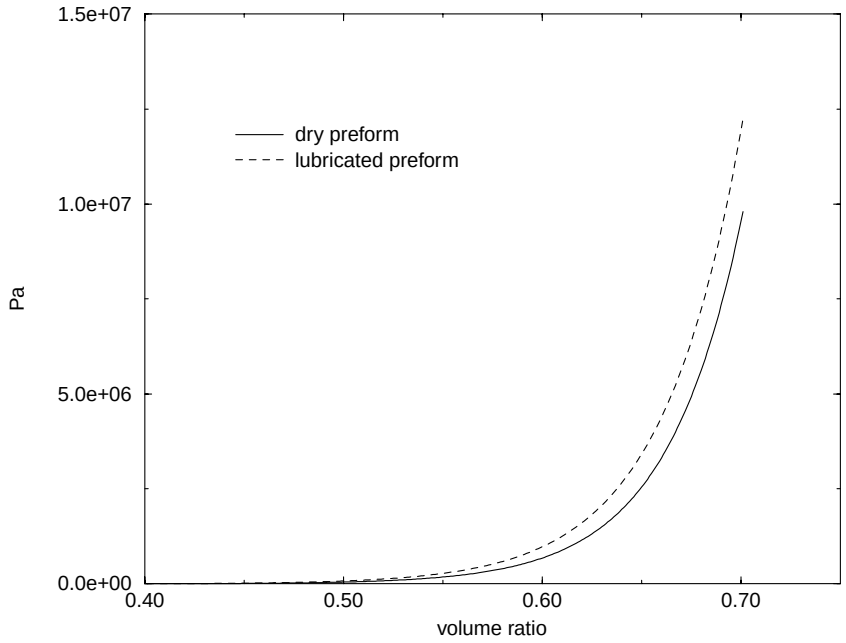

FIG. 2. *Stress–volume ratio relations for dry (G_s) and wet (G_m) preforms.*

where $\phi_r = 0.4$, $\beta = 0.09$ Pa, and $\gamma = 26.4$ in the wet region; $\beta = 0.3$ Pa and $\gamma = 25$ in the dry region, respectively. The permeability–volume relation is assumed to be given by

$$K(\phi) = K_0 e^{\alpha(\phi_1 - \phi)}, \tag{5.25}$$

where $\phi_1 = 0.6$, $K_0 = 10^{-9}\,\mathrm{m}^2$, $\alpha = 16$, well within the typical range specified, for instance, in [15] and [19]. The liquid is supposed to enter the porous medium at the constant velocity of $0.05\,\mathrm{ms}^{-1}$.

Figures 3–6 show the results of a simulation performed for $\mathcal{P} = 3 \cdot 10^{-6}$, $\mathcal{Q} = 0.5$, $\mathcal{L} = 2$, and $\mathcal{R} = 0.28$.

It is to be remarked that the very small nondimensional number $\mathcal{P}$, indicating a minor role played by the inertia, is to be considered really significant only when the solid has been largely infiltrated. In fact, the nondimensional numbers (5.7) have been obtained considering the equations driving the flow in the wet region of the preform. However, at the early times of the infiltration the preform is almost completely dry. The infiltration front $x_i(t)$ can be identified by looking at the point where the solution stops increasing and becomes flatter. Then there is no liquid pressure to be considered and in the equation of momentum there is only a balancing between the inertia of the solid and the stress in the solid itself. This is responsible for the rapid compression of the preform with nearly no infiltration.

The oscillations in the solid at the beginning of the infiltration, due to the initial conditions, may be seen in Figure 3, where the volume fraction in the porous preform can be compared at different times. It may be seen that the abrupt infiltration of the

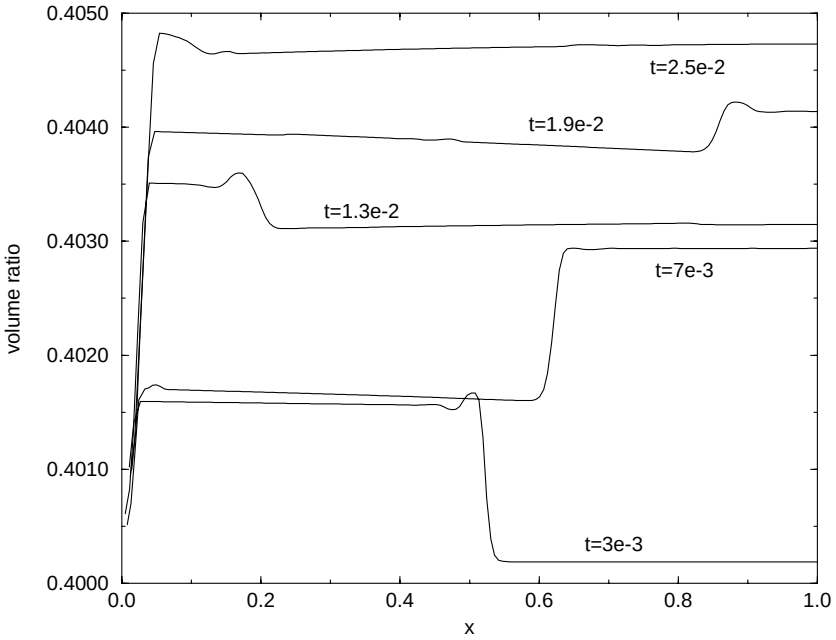

FIG. 3. *Volume ratio versus dimensionless space at different dimensionless times at the beginning of the infiltration process. During this period inertial terms are important, as is put into evidence by the compression–relaxation waves traveling back and forth in the dry region. Neglecting inertia would result in a constant volume ratio in such a region.*

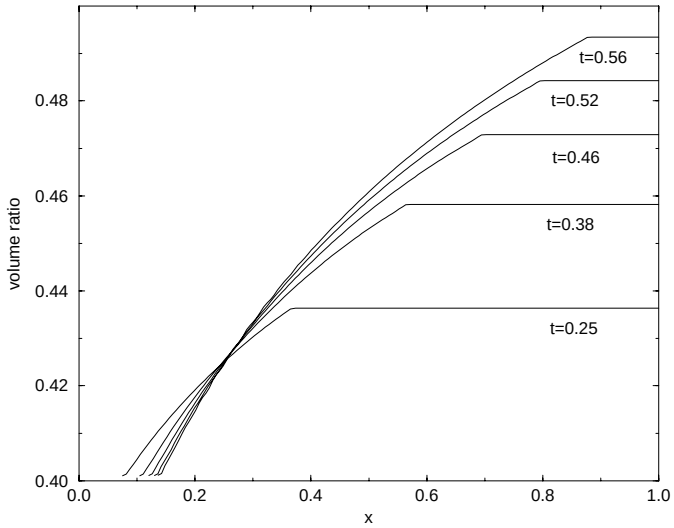

FIG. 4. *Volume ratio versus dimensionless space at different dimensionless times, later than in the previous plot. Now inertia is negligible, as can be deduced by the constant volume ratio computed in the dry region.*

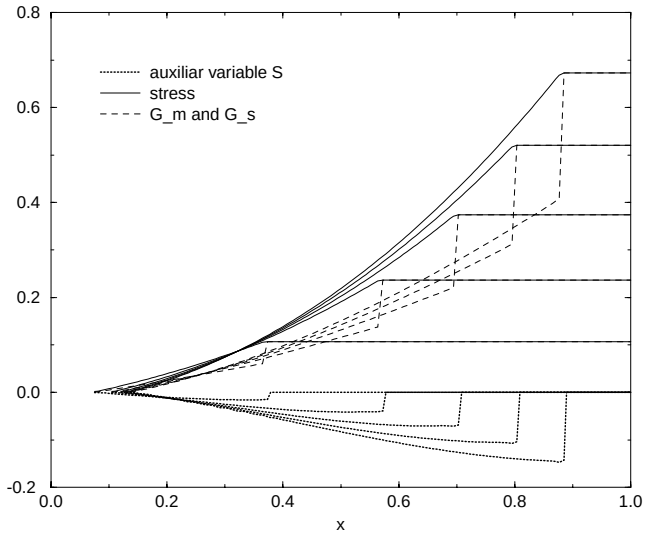

FIG. 5. *Stress measures versus dimensionless space at different dimensionless times.*

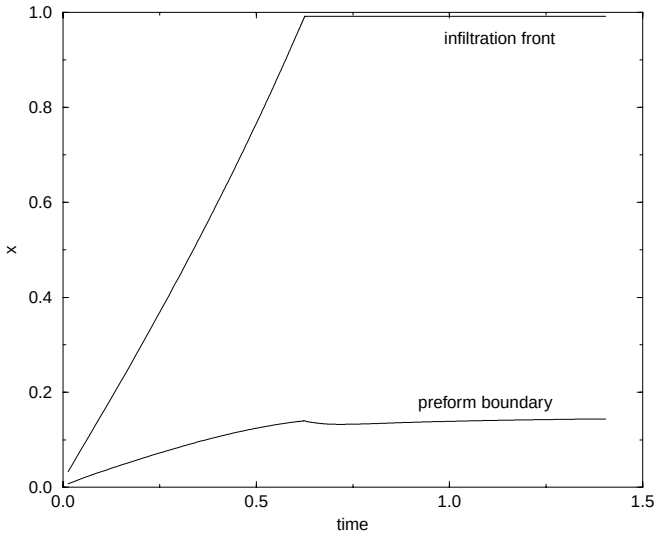

FIG. 6. *Evolution of the infiltration front x_i and of the preform boundary.*

resin at a given velocity causes the propagation of compression and relaxation waves in the dry elastic porous preform.

As time goes by, the oscillations due to initial conditions disappear and the advancing in time of the liquid boundary becomes clearly visible. Figure 4 gives the volume ratio displayed at different times when the liquid is advancing into the preform. The infiltration front is located at the discontinuity in slope. When comparing with Figure 3, it may be noticed that at later times inertia is negligible and, as a re-

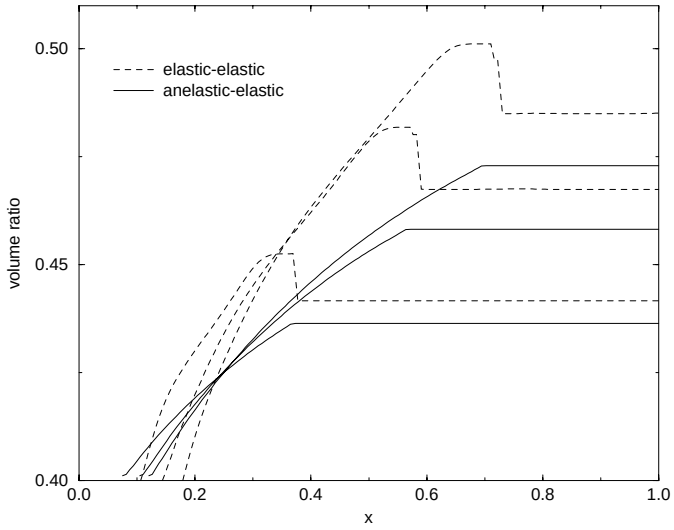

FIG. 7. *Comparison between the standard linear and the elastic cases. In the former case one has continuity of the volume ratio across the infiltration front. In the latter case the volume ratio is discontinuous across the infiltration front, with overcompression and corresponding stronger compression of the preform.*

sult, the volume ratio in the dry region is constant in space at a value corresponding to the pressure needed to push the liquid at the given inflow velocity. At the same moments, Figure 5 shows the curves corresponding to the stress, to G, and to the value of the auxiliary variable S_m. The different mechanical properties assumed to hold in the dry and wet regions of the preform yield a discontinuity of G at the liquid interface, while the stress is continuous.

Figure 6 shows the evolution of the infiltration front x_i and of the preform boundary x_f versus the dimensionless time. It may be seen that the interface advances in the preform at a nearly constant rate, because a constant inflow velocity of the liquid has been assumed. On the other hand, the material boundary can be seen to compress first and then relax after the infiltration has been completed. The preform is fully infiltrated at $t = 0.6 = 1 - \phi_0$ in agreement with a simple mass balance argument. Notice that the preform compresses under the action of the infiltration to about 84% of its rest length. After infiltration is completed, the preform relaxes slightly. Thanks to the elasticity and anelasticity assumptions it would relax completely if infiltration were stopped and spontaneous imbibition were allowed. However, this will not be possible in the presence of plastic phenomena, as would occur for most preforms.

Finally, Figure 7 shows a comparison between the case described above and the case of an elastic constitutive relationship holding for the whole preform, again obeying the same stress–strain relations given by G_m and G_s. As already mentioned, because of the reasons illustrated in section 4, in the elastic–elastic case the immediate response of the preform yields a discontinuity in the value of the volume ratio through the interface. The location of the preform border and the evolution of the volume ratio in the wet region is then very different, giving an overall compression after infiltration that is completed to about 80% the rest length. The evolution of the infiltration front and of the volume ratio in the wet region is instead only slightly affected.

6. Concluding remarks. A new mathematical model for the injection molding processes with deformable preforms has been derived in the framework of the theory of deformable porous media. The peculiar features of such a model are the assumption of nonnegligible inertia of the solid in the early times of the infiltration and the hypothesis that the preform obeys different stress–strain relationships depending on whether it is wet or dry. In particular, the preform has been assumed to behave as an elastic solid, when not yet infiltrated, while the mixture of the liquid and solid constituents is modeled as a standard linear solid. The set of equations governing the phenomena turns out to be typically of hyperbolic type. The two subdomains where different equations are defined deform in time, being separated by a moving interface. The mathematical problem is stiff in the sense that very different time scales are involved.

A numerical simulation of the injection molding process with a deformable porous preform has been performed in one dimension using a Godunov-type scheme with moving grids and a possibility of remeshing the domain. Although in the simulation inertia was considered at all times, it is evident that it plays an important role only to describe in a correct way the initial stages of the infiltration process. After a suitable interval of time, inertia could be dropped from the equations without losing accuracy and reducing the stiffness of the problem. This, however, leads to a change of type in the partial differential equations governing the system, calling for a different numerical approach.

The simulations presented show how the model can be used to determine the evolution of the deformation and stress state. As this can be helpful to quantify the inhomogeneous characteristics of the material and reveal in advance the possibility of damages in the reinforcing network, which may lead to material failure, one then has a tool to identify the parameter range to be used in the production cycle.

REFERENCES

[1] D. Purslow and R. Childs, *Autoclave moulding of carbon fibre-reinforced epoxies*, Composites, 17 (1986), pp. 127–136.

[2] L. Skartsis, J.L. Kardos, and B. Khomami, *Resin flow through fiber beds during composite manufacturing processes. Part* I: *Review of Newtonian flow through fiber beds*, Polymer Engrg. Sci., 32 (1992), pp. 221–230.

[3] R.K. Upadhyay and E.W. Liang, *Consolidation of advanced composites having volatile generation*, Polymer Compos., 16 (1995), pp. 96–108.

[4] V.M. Gonzalez-Romero and C.W. Macosko, *Process parameters estimation for structural reaction injection molding and resin transfer molding*, Polymer Engrg. Sci., 30 (1990), pp. 142–146.

[5] K. Han, L.J. Lee, and M.J. Liou, *Fiber mat deformation in liquid composite molding.* II: *Modeling*, Polymer Compos., 14 (1993), pp. 151–160.

[6] K. Han, L. Trevino, L.J. Lee, and M.J. Liou, *Fiber mat deformation in liquid composite molding.* I: *Experimental analysis*, Polymer Compos., 14 (1993), pp. 144–150.

[7] Y.R. Kim, S.P. McCarthy, and J.P. Fanucci, *Compressibility and relaxation of fiber reinforcements during composite processing*, Polymer Compos., 12 (1991), pp. 13–19.

[8] E. Lacoste, M. Aboulfatah, M. Danis, and F. Girot, *Numerical simulation of the infiltration of fibrous preforms by a pure metal*, Metall. Trans. A, 24 (1993), pp. 2667–2678.

[9] E. Lacoste, M. Danis, F. Girot, and J.M. Quennisset, *Numerical simulation of the injection moulding of thin parts by liquid metal infiltration of fibrous preform*, Mater. Sci. Engrg. A, 135 (1991), pp. 45–49.

[10] C. Lekakou, M.A.K.B. Johari, and M.G. Bader, *Compressibility and flow permeability of two dimensional woven reinforcements in the processing of composites*, Polymer Compos., 17 (1996), pp. 666–672.

[11] A. Mortensen and T. Wong, *Infiltration of fibrous preforms by a pure metal: Part* III. *Capillary phenomena*, Metall. Trans. A, 21 (1990), pp. 2257–2263.

[12] J.D. Nam, J.C. Seferis, S.W. Kim, and K.J. Lee, *Gas permeation and viscoelastic deformation of prepregs in composite manufacturing processes*, Polymer Compos., 16 (1995), pp. 370–377.
[13] C.D. Rudd and K.N. Kendall, *Towards a manufacturing technology for high-volume production of composite components*, Proc. Inst. Mech. Engrs., 206 (1992), pp. 77–91.
[14] C.D. Rudd, M.J. Owen, and V. Middleton, *Effects of process variables on cycle time during resin transfer moulding for high volume manufacture*, Mater. Sci. Tech., 6 (1990), pp. 656–665.
[15] J.L. Sommer and A. Mortensen, *Forced unidirectional infiltration of deformable porous media*, J. Fluid Mech., 311 (1996), pp. 193–215.
[16] L. Trevino, K. Rupel, W.B. Young, M.J. Liou, and L.J. Lee, *Analysis of resin injection molding in molds with preplaced fiber mats.* I: *Permeability and compressibility measurements*, Polymer Compos., 12 (1991), pp. 20–29.
[17] T. Yamauchi and Y. Nishida, *Infiltration kinetics of fibrous preforms by aluminum with solidification*, Acta Metall. Mater., 43 (1995), pp. 1313–1321.
[18] W.B. Young and C.W. Chiu, *Study of compression transfer molding*, J. Compos. Mater., 29 (1995), pp. 2180–2191.
[19] W.B. Young, K. Rupel, K. Han, L.J. Lee, and M.J. Liou, *Analysis of resin injection molding in molds with preplaced fiber mats.* II: *Numerical simulation and experiments of mold filling*, Polymer Compos., 12 (1991), pp. 30–38.
[20] L. Preziosi, *The theory of deformable porous media and its application to composite material manufacturing*, Surveys Math. Indust., 6 (1996), pp. 167–214.
[21] L. Preziosi, D.D. Joseph, and G.S. Beavers, *Infiltration in initially dry, deformable porous media*, Internat. J. Multiphase Flows, 22 (1996), pp. 1205–1222.
[22] D. Ambrosi and L. Preziosi, *Modelling matrix injection through porous preforms*, Composites, Part A, 29 (1998), pp. 5-18.
[23] L. Billi and A. Farina, *Unidirectional infiltration in deformable porous media: Mathematical modelling and self-similar solution*, Quart. Appl. Math., 58 (2000) pp. 85–101.
[24] K.R. Rajagopal and L. Tao, *Mechanics of Mixtures*, World Scientific, London, Singapore, 1995.
[25] R.M. Bowen, *Incompressible porous media models by use of the theory of mixtures*, Internat. J. Engrg. Sci., 18 (1980), pp. 1129–1148.
[26] L. Tao, K. R. Rao, and A.S. Wineman, *Unsteady diffusion of fluids through solids undergoing large deformations*, Math. Models Methods Appl. Sci., 1 (1991), pp. 311–346.
[27] T.G. Gutowski, *A resin flow–fiber deformation model for composites*, SAMPE Quart., 16 (1985), pp. 58–64.
[28] M. Hassanizadeh and W.G. Gray, *General Balance Equations for Multiphase Systems*, Princeton University Press, Princeton, NJ, 1978.
[29] J. H. Prevost, *Mechanics of continuous porous media*, Internat. J. Engrg. Sci., 18 (1980), pp. 787–800.
[30] J.S. Hou, M.H. Holmes, W.M. Lai, and V.C. Mow, *Boundary conditions at the cartilage-synovial fluid interface for joint lubrication and theoretical verification*, J. Biomech. Engrg., 111 (1989), pp. 78–87.
[31] I.S. Liu, *On chemical potential and incompressible porous media*, J. Mécanique, 19 (1980), pp. 327–342.
[32] I. Müller, *Thermodynamics of mixtures of fluids*, J. Mécanique, 14 (1975), pp. 267–303.
[33] M. Vinokur, *An analysis of finite-difference and finite-volume formulations of conservation laws*, J. Comput. Phys., 81 (1989), pp. 1–52.
[34] R.J. LeVeque, *Numerical Methods for Conservation Laws*, Birkhäuser-Verlag, Zurich, 1992.
[35] N. Bellomo and L. Preziosi, *Modelling Mathematical Methods and Scientific Computation*, CRC Press, Boca Raton, FL, 1995.
[36] L. Tao and K. R. Rajagopal, *On boundary conditions in mixture theory*, in Recent Advances in Elasticity Viscoelasticity and Inelasticity, K.R. Rajagopal, ed., World Scientific, River Edge, NJ, 1995, pp. 130–149.
[37] U. Hornung, *Homogenization and Porous Media*, Springer, Berlin, 1997.
[38] W. Jäger and A. Mikelic, *On the boundary conditions at the contact interface between a porous medium and a free fluid*, Ann. Scuola Norm. Sup. Pisa Cl. (4), 23 (1996), pp. 403–465.